Millimeter-Wave Human Blockage at 73 GHz and Millimeter-Wave Diffraction at 10, 20 and 26 GHz

NYU WIRELESS WebEx

George R. MacCartney Jr., Theodore S. Rappaport, Sijia Deng, and Shu Sun

{gmac,sijia,ss7152,tsr}@nyu.edu

- G. R. MacCartney, Jr., S. Deng, S. Sun, and T. S. Rappaport, "Millimeter-Wave Human Blockage at 73 GHz with a Simple Double Knife-Edge Diffraction Model and Extension for Directional Antennas," *2016 IEEE 84th Vehicular Technology Conference: VTC2016-Fall*, Montreal, Canada, Sept. 2016.
- S. Deng, G. R. MacCartney, Jr., and T. S. Rappaport, "Millimeter Wave Diffraction Measurements and Models at 10, 20, and 30 GHz," *2016 IEEE Global Communications Conference (GLOBECOM)*, Washington, D.C., USA, Dec. 2016.

Human Blockage Agenda

- **Human Blockage in Channel Models**
- **Knife-Edge Diffraction Models**
- **Measurement System and Specifications**
- **Measurement Environment, Setup, and Test Description**
- **Measurement Results**
- **Observations and Conclusions**

Millimeter Wave Diffraction Measurements

- Develop accurate human blocking model
- Gain insight into phenomenon of diffraction around objects at millimeter-wave (mmWave) bands in indoor and outdoor environments
- Investigate effects of environment, material type and object shape
- Develop accurate and simple diffraction loss models
- Evaluate the applicability of the Knife Edge Diffraction (KED) model at mmWave bands

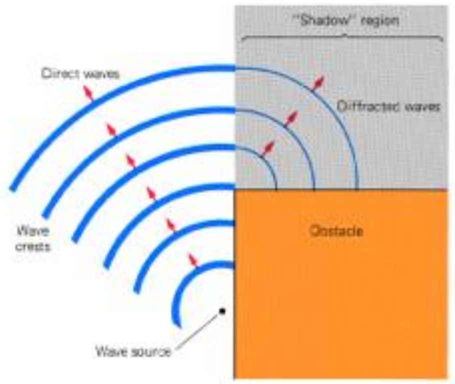

T. S. Rappaport, Wireless Communications: Principles and Practice, 2nd ed. Upper Saddle River, NJ: Prentice Hall, 2002.
K. B. Krauskopf, A. Beiser, The Physical Universe, McGraw Hill, 2002.

NYU TANDON SCHOOL OF ENGINEERING

Human Blockage

NYU WIRELESS

- **Human blockage models did not exist in early 3GPP standards**
- **Millimeter-wave (mmWave) requires narrow beams with beamforming**
- **Human blocking causes dynamic deep fades at mmWave**
- **Diffraction is more lossy at mmWave compared to sub-6 GHz frequencies**
- **Recent standards have incorporated human blockage models:**
  - **IEEE 802.11ad**
  - **Mobile and wireless communications enablers for the twenty-twenty information society (METIS)**
  - **3rd Generation Partnership Project (3GPP) TR 38.900 (Release 14)**

A. Maltsev, et al., “Channel models for 60 GHz WLAN systems,” IEEE doc. 802.11-09/0334r4

METIS2020, “METIS Channel Model,” Tech. Rep. METIS2020, Deliverable D1.4 v3, July 2015. [Online]. Available: https://www.metis2020.com/wp-content/uploads/deliverables/METIS_D1.4_v1.0.pdf

3GPP, “Technical specification group radio access network; channel model for frequency spectrum above 6 GHz,” 3rd Generation Partnership Project (3GPP), TR 38.900, June. 2016. [Online]. Available: http://www.3gpp.org/DynaReport/38900.htm

IEEE 802.11ad Human Blockage

- Statistical distributions used to simulate human blockage for: decay time, rise time, duration, and mean attenuation
- Mostly ray-tracing simulations and few measurements used to create the model

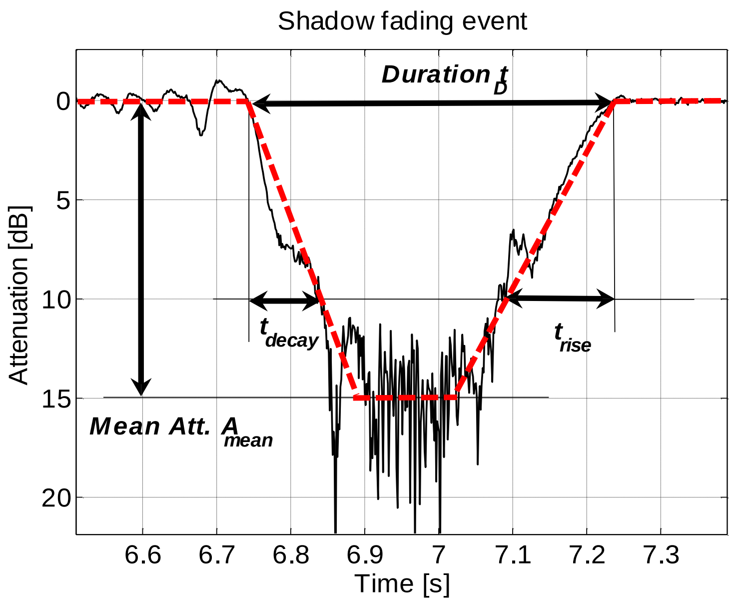

Figure from: A. Maltsev, et al., "Channel models for 60 GHz WLAN systems," IEEE doc. 802.11-09/0334r8

METIS Human Blockage

- Human walking in front of antennas at 60 GHz for a 4 m T-R separation distance
- Limited measurements compared to model for validation
- Approximation of knife-edge diffraction (KED) from multiple edges used for model
  - Originally based on measurements with dipole antennas (omnidirectional)

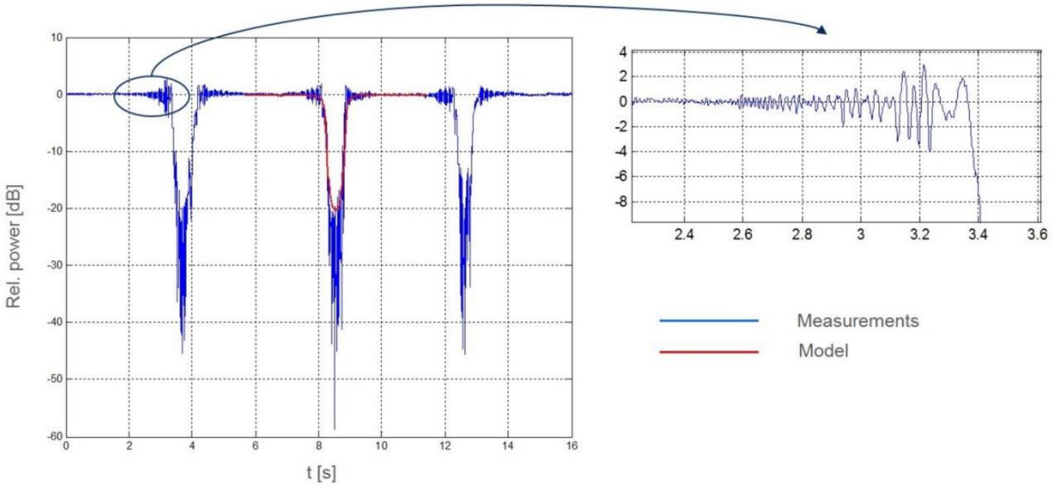

- METIS2020, "METIS Channel Model," Tech. Rep. METIS2020, Deliverable D1.4 v3, July 2015. [Online]. Available: https://www.metis2020.com/wp-content/uploads/deliverables/METIS_D1.4_v1.0.pdf
- J. Medbo and F. Harrysson, "Channel modeling for the stationary UE scenario," Antennas and Propagation (EuCAP), 2013 7th European Conference on, Gothenburg, 2013, pp. 2811-2815.

2D and 3D Knife-Edge Diffraction in METIS

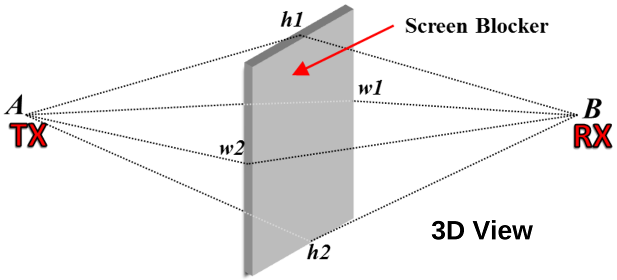

3D View

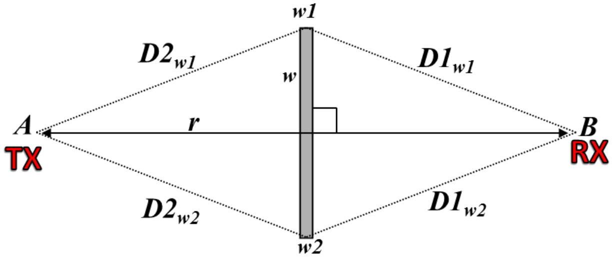

Top-down View

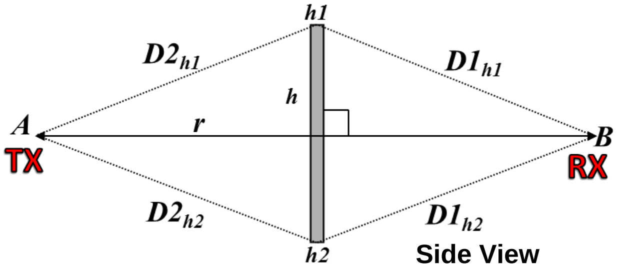

Side View

METIS blockage model

F = E-field gain due to diffraction

$F_{w1}|_{w2} = F_{w1}$ or F_{w2}

- Shadowing by 4 screen edges:

$$F_{w1|w2} = \frac{\tan^{-1}\left(\pm\frac{\pi}{2}\sqrt{\frac{\pi}{\lambda}(D2_{w1|w2} + D1_{w1|w2} - r)}\right)}{\pi}$$

$$F_{h1|h2} = \frac{\tan^{-1}\left(\pm\frac{\pi}{2}\sqrt{\frac{\pi}{\lambda}(D2_{h1|h2} + D1_{h1|h2} - r)}\right)}{\pi}$$

where for $\pm$, the plus (+) indicates the shadow zone and the minus (-) indicates the LOS zone. For a region where there is a clear LOS, the edge closest to the LOS is considered the LOS zone and the edge farthest from the LOS is considered the shadow zone (see next slide).

- KED Shadowing loss (four edges):

$$L_{\text{screen}}[\text{dB}] = -20\log_{10}\left(1 - (F_{h1} + F_{h2})(F_{w1} + F_{w2})\right)$$

- Double knife-edge diffraction (DKED) shadowing loss (2D, infinitely high screen) :

$$L_{\text{screen}}[\text{dB}] = -20\log_{10}\left(1 - (F_{w1} + F_{w2})\right)$$

METIS2020, “METIS Channel Model,” Tech. Rep. METIS2020, Deliverable D1.4 v3, July 2015. [Online]. Available: https://www.metis2020.com/wp-content/uploads/deliverables/METIS_D1.4_v1.0.pdf

2D and 3D Knife-Edge Diffraction in METIS

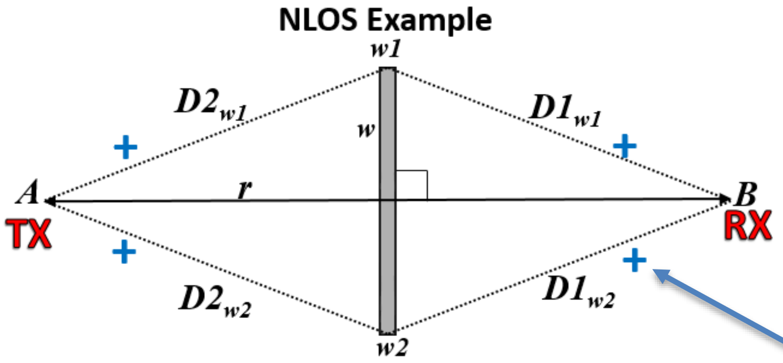

How to apply **+/-** to edges in KED equation

$$F_{w1|w2} = \frac{\tan^{-1}\left(\pm\frac{\pi}{2}\sqrt{\frac{\pi}{\lambda}(D2_{w1|w2}+D1_{w1|w2}-r)}\right)}{\pi}$$

$$F_{h1|h2} = \frac{\tan^{-1}\left(\pm\frac{\pi}{2}\sqrt{\frac{\pi}{\lambda}(D2_{h1|h2}+D1_{h1|h2}-r)}\right)}{\pi}$$

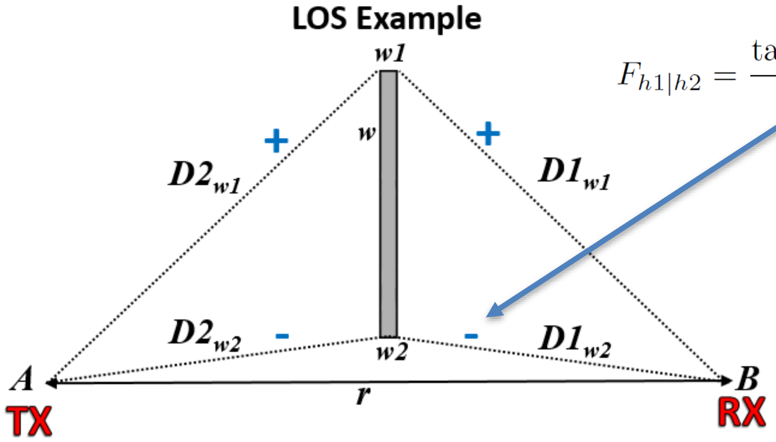

3GPP, "Technical specification group radio access network; channel model for frequency spectrum above 6 GHz," 3rd Generation Partnership Project (3GPP), TR 38.900, June. 2016. [Online]. Available: http://www.3gpp.org/DynaReport/38900.htm

METIS2020, "METIS Channel Model," Tech. Rep. METIS2020, Deliverable D1.4 v3, July 2015. [Online]. Available: https://www.metis2020.com/wp-content/uploads/deliverables/METIS_D1.4_v1.0.pdf

3D Knife-Edge Diffraction in 3GPP

- 3GPP has two different KED human blockage models
  - Model A: based on polar coordinates, but similar to METIS (see page 48 of 3GPP TR 38.900 V14.0.0)
  - Model B: based on Cartesian coordinates and identical to the METIS model (see page 50 of 3GPP TR 38.900 V14.0.0)

3GPP, "Technical specification group radio access network; channel model for frequency spectrum above 6 GHz," 3rd Generation Partnership Project (3GPP), TR 38.900, June. 2016. [Online]. Available: http://www.3gpp.org/DynaReport/38900.htm

METIS2020, "METIS Channel Model," Tech. Rep. METIS2020, Deliverable D1.4 v3, July 2015. [Online]. Available: https://www.metis2020.com/wp-content/uploads/deliverables/METIS_D1.4_v1.0.pdf

Human blockage with directional antennas

- Neither METIS or 3GPP account for high gain antennas
- High gain antennas do not have uniform gain across a human blocker or screen
- This error is large (>10 dB) when the human blocker is close to TX or RX (0.5 to 1.5 meters)

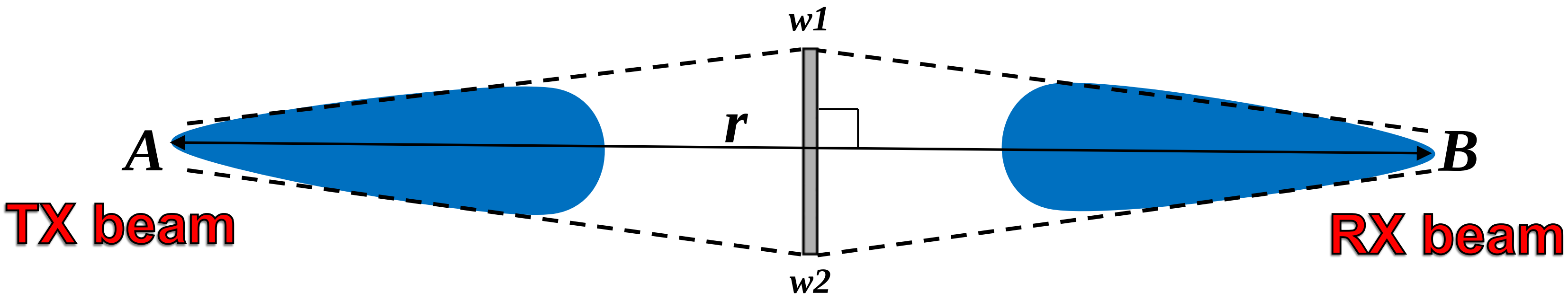

Proposed Double Knife-Edge Diffraction (DKED) Model Extension for Directional Antennas

- We used antenna radiation patterns to extend the 2D METIS DKED model to account for non-uniform gain:

$$L_{\text{Screen Mod.}}[\text{dB}] = -20\log_{10}\left|\left(\frac{1}{2}-F_{w1}\right)\cdot\sqrt{G_{D2_{w1}}}\cdot\sqrt{G_{D1_{w1}}}+\left(\frac{1}{2}-F_{w2}\right)\cdot\sqrt{G_{D2_{w2}}}\cdot\sqrt{G_{D1_{w2}}}\right|$$

$G_{D2w1|D1w1|D2w2|D1w2}$ are the normalized linear gains of the TX and RX antennas
$D2_{w1|w2}$ and $D1_{w1|w2}$ are the projected distances from the TX to the screen edge and from the screen to the RX, respectively.
.

Normalized azimuth gain (G) at angle θ is determined via far-field radiation pattern with azimuth half-power beamwidth, $HPBW_{AZ}$:

where:

$$G(\theta) = \text{sinc}^2(\text{a}\cdot\sin(\theta))\cdot\cos^2(\theta)$$

$$\text{sinc}^2\left(\text{a}\cdot\sin\left(\frac{\text{HPBW}_{\text{AZ}}}{2}\right)\right)\cdot\cos^2\left(\frac{\text{HPBW}_{\text{AZ}}}{2}\right)=\frac{1}{2}$$

S. Sun, G. R. MacCartney, Jr., M. K. Samimi, and T. S. Rappaport, “Synthesizing omnidirectional antenna patterns, received power and path loss from directional antennas for 5g millimeter-wave communications,” in *2015 IEEE Global Communications Conference (GLOBECOM)*, Dec. 2015, pp. 1–7.

Far field radiation from electric current. [Online]. Available: http://www.thefouriertransform.com/applications/radiation.php

Measurement System Specifications

Description	Specification
Baseband Sequence	PRBS (11th order: 2^{11}-1 = Length 2047)
Chip Rate	500 Mcps
RF Null-to-Nulll Bandwidth	1 GHz
PDP Detection	FFT matched filter
Sampling Rate	1.5 GS/s *I* and *Q*
Multipath Time Resolution	2 ns
Minimum Periodic PDP Interval	32.752 μs
Maximum Frequency Interval	30.053 kHz (±15.2 kHz max Doppler)
Maximum Periodic PDP records per snapshot	41,000 PDPs
PDP Threshold	25 dB down from max peak
TX/RX Intermediate Frequency	5.625 GHz
TX/RX LO	67.875 GHz (22.625 GHz x3)
Synchronization	TX/RX Share 10 MHz Reference
Carrier Frequency	73.5 GHz
TX Power	-5.8 dBm
TX/RX Antenna Gain	20 dBi
TX/RX Azimuth and Elevation HPBW	15º
TX/RX Antenna Polarization	V-V
EIRP	14.2 dBm
TX/RX Heights	1.4 m

- Real-time spread spectrum sequence wideband correlator channel sounder
- Measurement specific details:
  - 5 second capture window that records 500 PDPs/second (2500 total PDPs)

TX

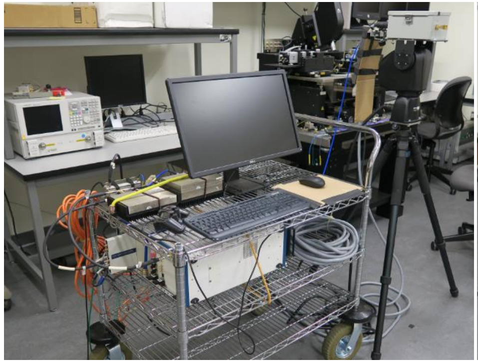

RX

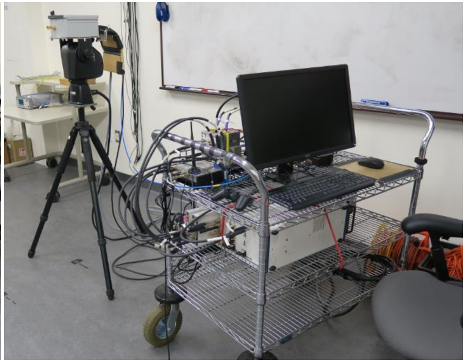

G. R. MacCartney, Jr., S. Deng, S. Sun, and T. S. Rappaport, "Millimeter-Wave Human Blockage at 73 GHz with a Simple Double Knife-Edge Diffraction Model and Extension for Directional Antennas," *2016 IEEE 84th Vehicular Technology Conference: VTC2016-Fall*, Montreal, Canada, Sept. 2016.

Measurement Environment / Setup

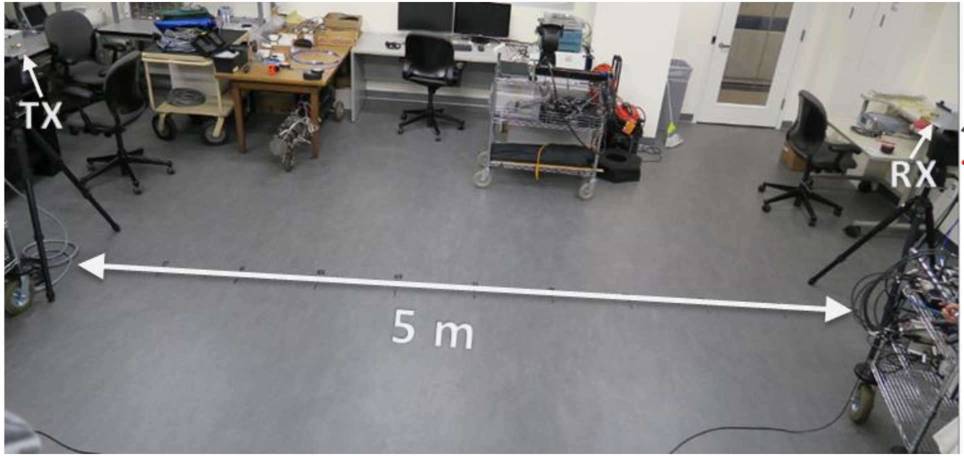

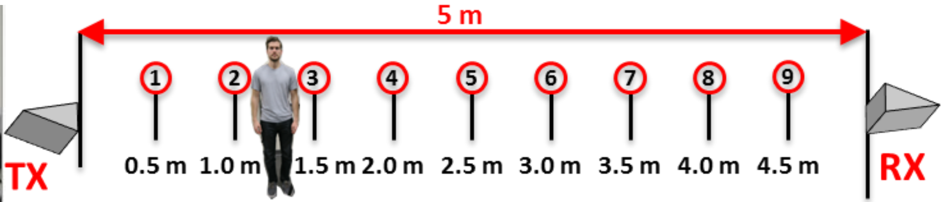

- Measurements for a T-R separation distance of 5 m for 9 discrete blockage positions between the TX and RX from 0.5 m to 4.5 m in 0.5 m increments
- Fraunhofer distance of antennas at 73.5 GHz: 0.292 m
- Human blocker moves at approximate speed of 1 m/s with body depth (0.28 m) blocking LOS.

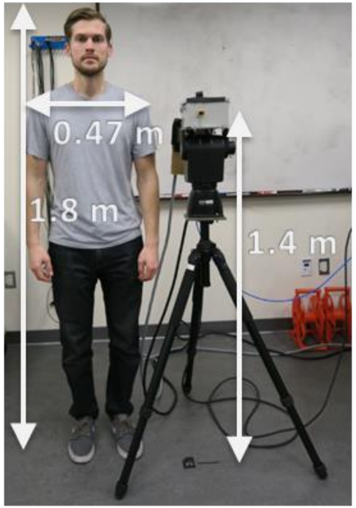

Human Blockage Measurements Compared to DKED Models

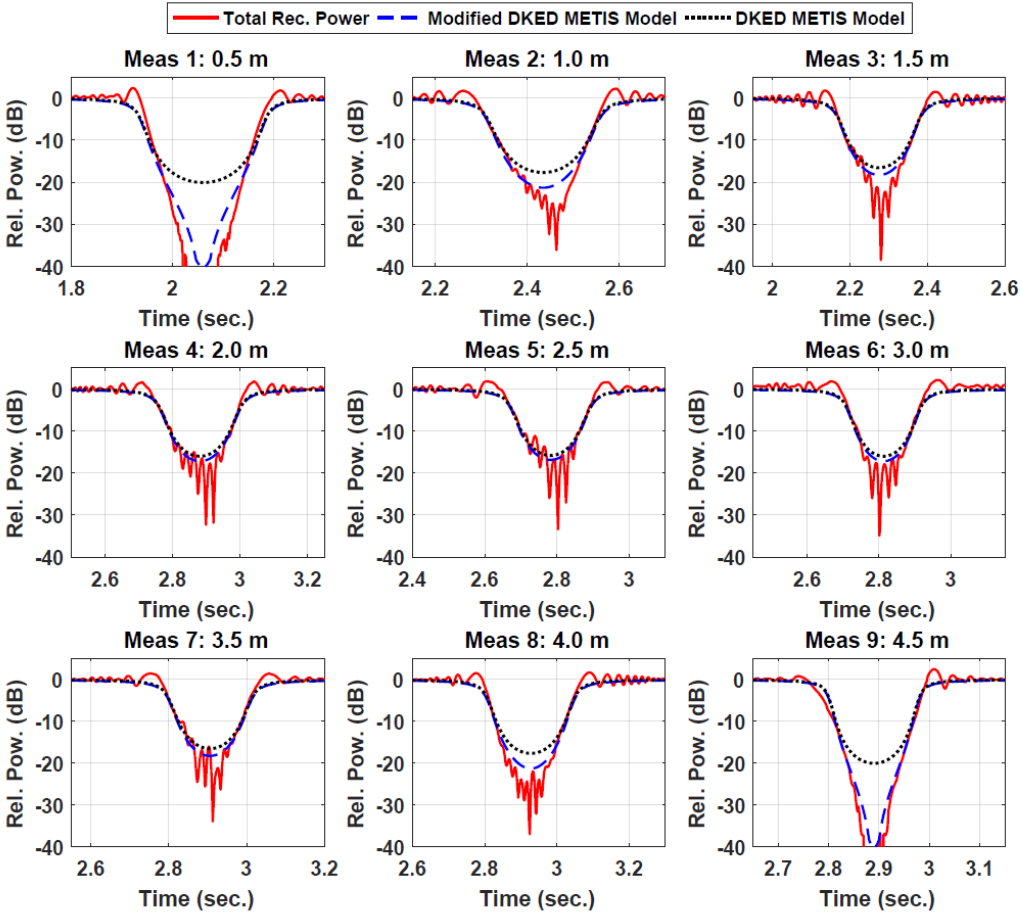

- **DKED 3GPP/METIS model does not match the measurement results in the deep shadow region, predicting less loss than observed.**
- **Our proposed DKED model with antenna gains matches well with the upper envelope of the shadowing loss**
- **Narrowbeam antennas cause greater diffraction loss from blockers, with deeper fades in the shadow region, compared to the DKED omnidirectional antenna model.**
- **Better prediction of diffraction loss when close to TX or RX antenna**

G. R. MacCartney, Jr., S. Deng, S. Sun, and T. S. Rappaport, "Millimeter-Wave Human Blockage at 73 GHz with a Simple Double Knife-Edge Diffraction Model and Extension for Directional Antennas," *2016 IEEE 84th Vehicular Technology Conference: VTC2016-Fall*, Montreal, Canada, Sept. 2016.

Prediction in Deep Shadow Region

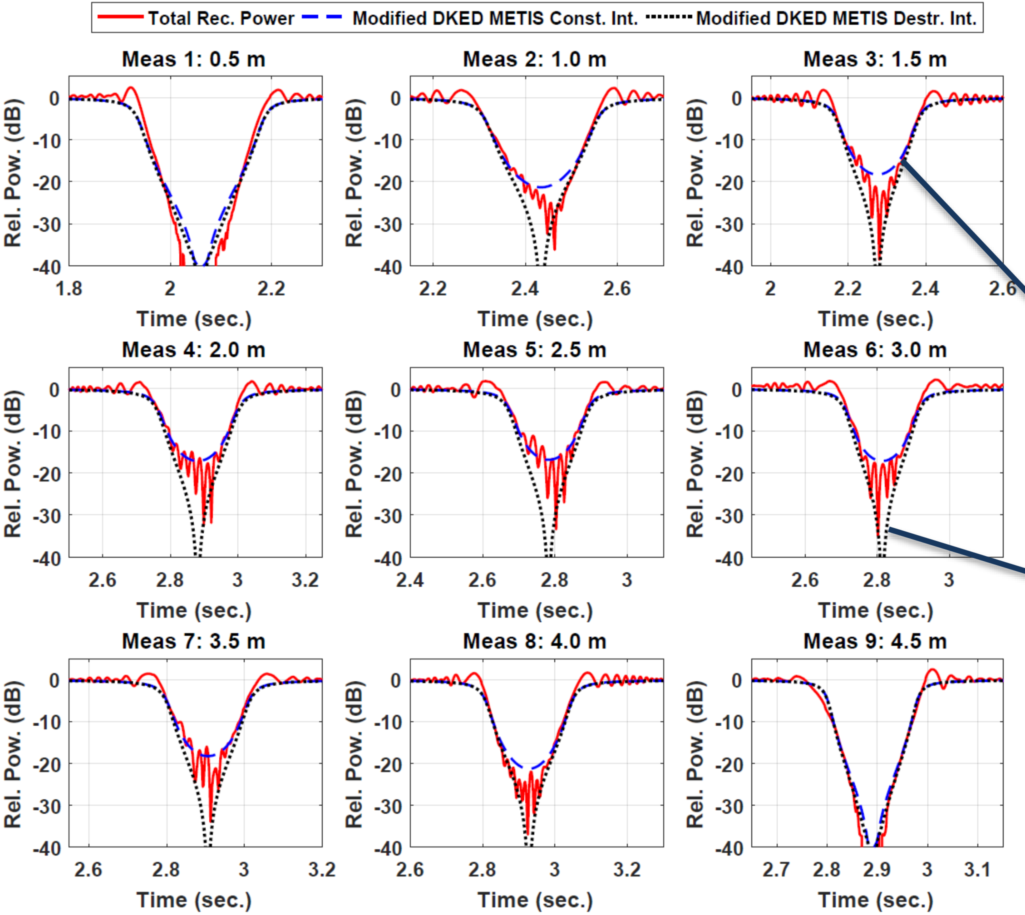

- Our modified DKED model that includes antennas gains at screen edges and with coherent ***sum of fields*** from both edges matches the upper bound envelope of the total received power deep shadowing, representing **constructive interference**
- Our modified DKED model that includes antennas gains at screen edges and with coherent ***difference of fields*** from both edges matches the lower bound envelope of the total received power deep shadowing, representing **destructive interference**

- M. Jacob et al., "A ray tracing based stochastic human blockage model for the IEEE 802.11ad 60 GHz channel model," Proceedings of the 5th European Conference on Antennas and Propagation (EUCAP), Rome, 2011, pp. 3084-3088.
- G. R. MacCartney, Jr., S. Deng, S. Sun, and T. S. Rappaport, "Millimeter-Wave Human Blockage at 73 GHz with a Simple Double Knife-Edge Diffraction Model and Extension for Directional Antennas," *2016 IEEE 84th Vehicular Technology Conference: VTC2016-Fall*, Montreal, Canada, Sept. 2016.

Observations and Conclusion

- **Shadowing events lasted between approximately 200 and 300 ms on average**
- **Reciprocal shadowing observations made at either TX/RX measurement locations such as 0.5 meters from the TX (Meas 1) and 0.5 meters from the RX (Meas 9)**
- **Deep fades (maximum attenuation) during shadowing could exceed 40 dB. Less loss when blocker was further from the TX and RX (Meas 5, 2.5 m from both TX and RX).**
- **Our modified DKED model with antenna gains can be used to determine minimum and maximum fade depths caused by human blockage**
- **Temporal variations and large shadowing events can be overcome by beamsteering to find scatterers and reflections to improve SNR.**

Diffraction Agenda

- **Millimeter Wave Diffraction Measurements at 10, 20, and 26 GHz**
- **Diffraction Measurement System and Procedures**
- **Indoor and Outdoor Measurement Environment and Measured Materials**
- **KED Model and Creeping Wave Linear Model**
- **Indoor and Outdoor Measurement Results**
- **Measurement Result Use Cases**
- **Conclusion**

Indoor Diffraction Measurement Material

Three measurement materials: Drywall Corner, Plastic Board, and Wooden Corner

Plastic Board

Semi-transparent board with a thickness of 2 cm

Wooden Corner

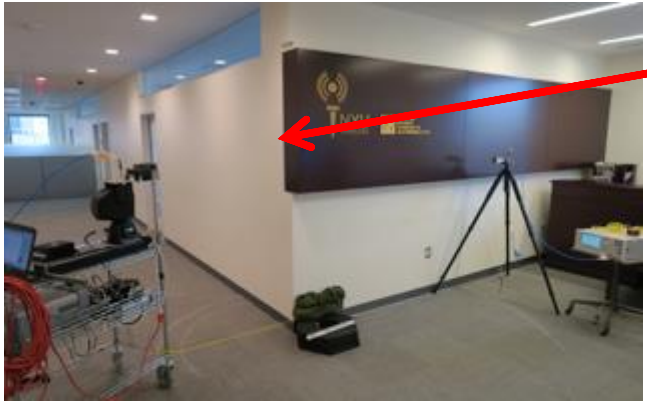

Drywall Corner

Vertical metal stud inside

Drywall Corner

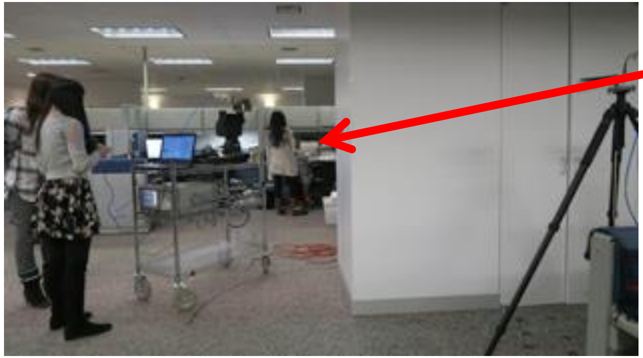

Outdoor Diffraction Measurements

Two measurement locations: Marble Corner and Stone Pillar

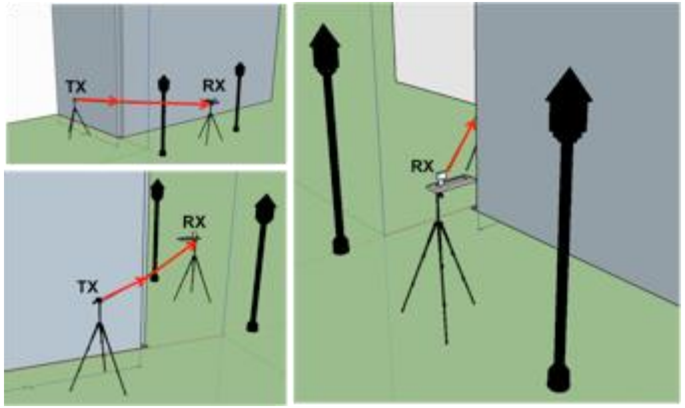

Rough Surface with rounded corners

Measurement Procedure

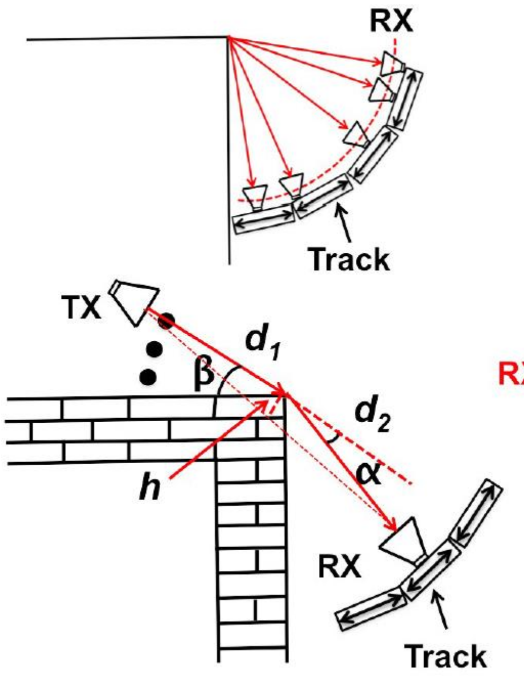

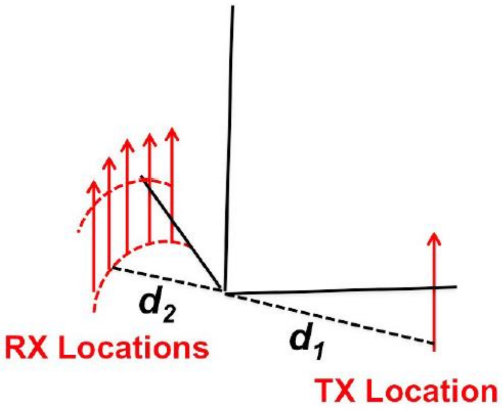

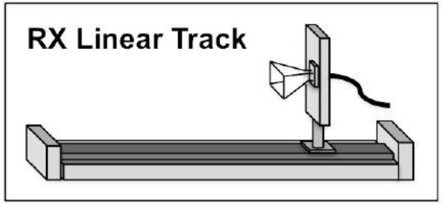

- **Three** TX incidence angles per material (indoor)
- **Two** TX incidence angles per material (outdoor)
- **Five** RX track locations, RX antenna moves in 8.75 mm increments (corresponding to 0.5º increments) from NLOS to LOS environment
- **40** Measurements per track, **200** total data points for each TX incident angle

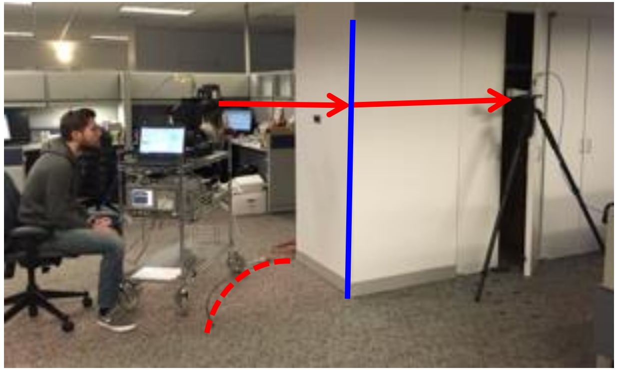

Knife Edge Diffraction Model

Knife Edge Diffraction Model (KED)

$$\frac{E_{\text{KED}}}{E_0} = F(u) = \frac{1+j}{2} \cdot \int_u^{\infty} e^{-j(\pi/2)t^2}\,dt$$

$$u = u\sqrt{\frac{2(d_1+d_2)}{\lambda d_1 d_2}} = \alpha\sqrt{\frac{2d_1d_2}{\lambda(d_1+d_2)}}$$

$$G(u)[\text{dB}] = -P(u) = 20\log_{10}|F(u)|$$

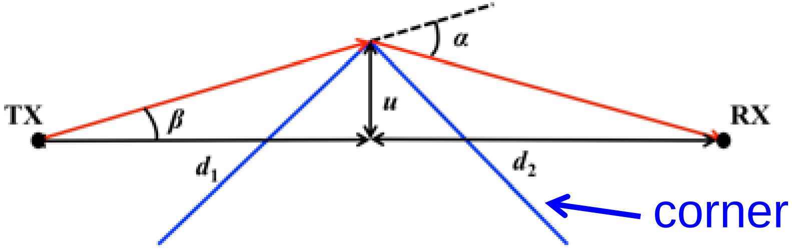

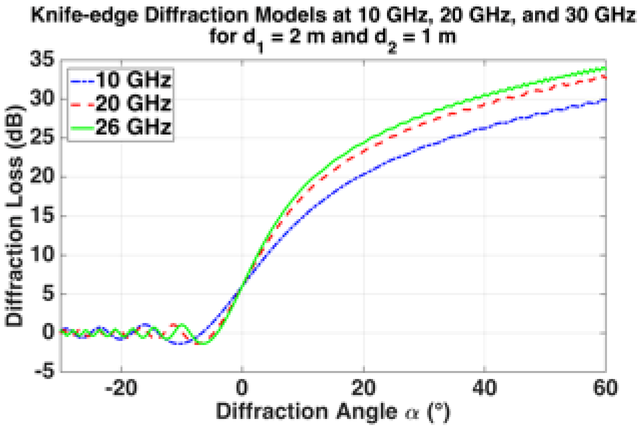

A Function of Frequency and Diffraction Angle

T. S. Rappaport, Wireless Communications: Principles and Practice, 2nd ed. Upper Saddle River, NJ: Prentice Hall, 2002.

Creeping Wave Linear Model

Linear Model with fixed anchor point

$$E \sim E_i e^{-jk\alpha R_h} \frac{e^{-jkd_2}}{\sqrt{kd_2}} \sum_{p=1}^{\infty} D_p R_h \exp(-\psi_p \alpha)$$

$$\frac{E}{E_i} \sim D_p R_h \exp(-\psi_p \alpha)$$

$$D_p, R_h \sim \left(\frac{kP_h}{2}\right)^{\frac{1}{3}}$$

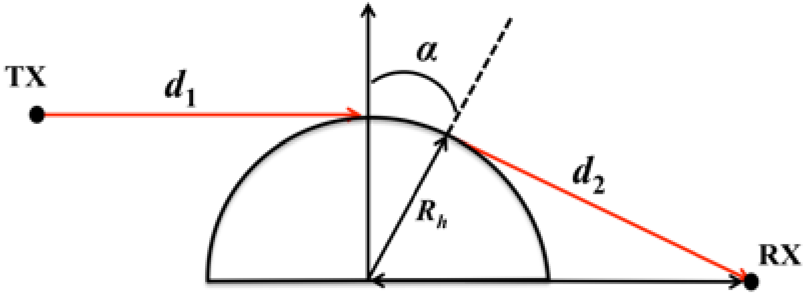

E_i **Incident field**

k **Wave number**

D_p **Excitation coefficient**

ψ_p **Attenuation constant**

$$G(\alpha)[\text{dB}] = -P(\alpha) = 20\log_{10} E = -A(R_h, f)\psi_p \alpha + C(R_h, f)$$

$$P(\alpha) = n\alpha + c$$

A function of diffraction angle (α)

c = 6 dB

L. Piazzi and H. L. Bertoni, "Effect of terrain on path loss in urban environments for wireless applications," IEEE Transactions on Antennas and Propagation, vol. 46, no. 8, pp. 1138-1147, Aug. 1998.

Drywall KED Measurements Results

Free Space Transmission, Reflection, and Diffraction

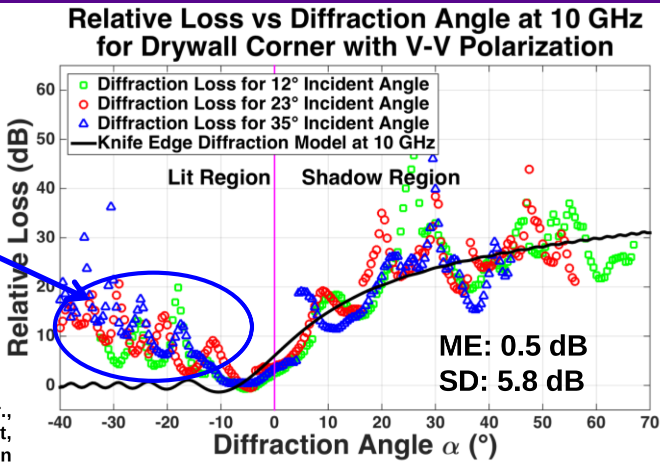

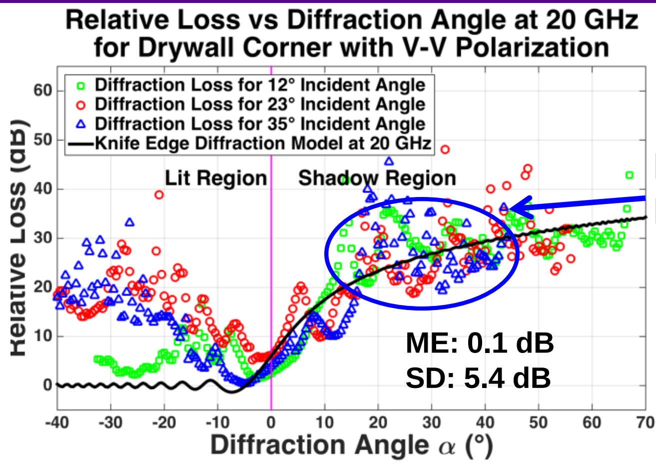

Diffraction and Penetration

S. Deng, G. R. MacCartney, Jr., and T. S. Rappaport, "Millimeter Wave Diffraction Measurements and Models at 10, 20, and 30 GHz," *2016 IEEE Global Communications Conference (GLOBECOM)*, Dec. 2016.

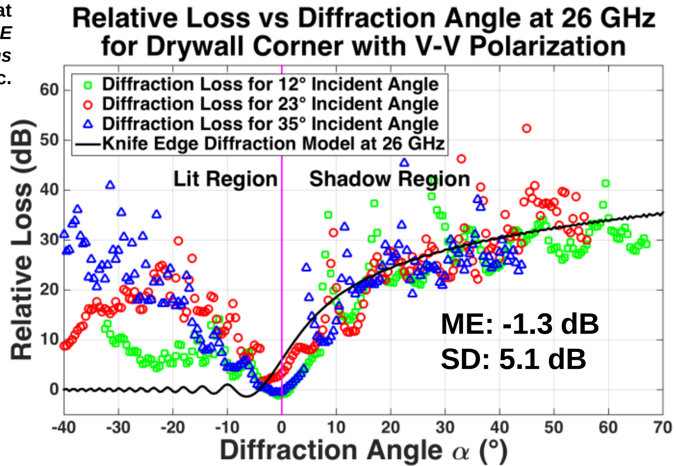

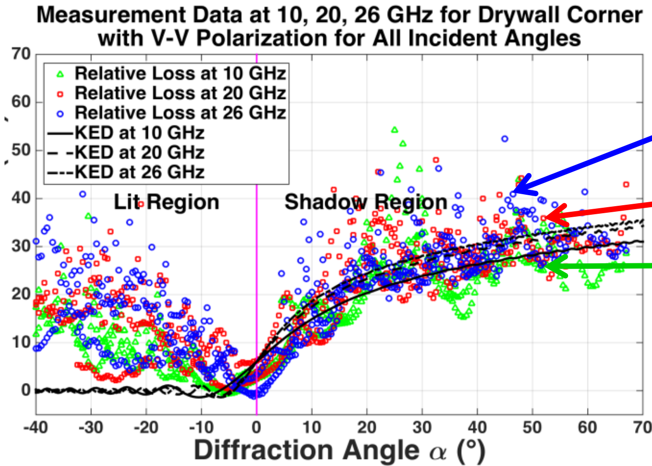

26 GHz

20 GHz

10 GHz

Wooden Corner KED Measurements Results

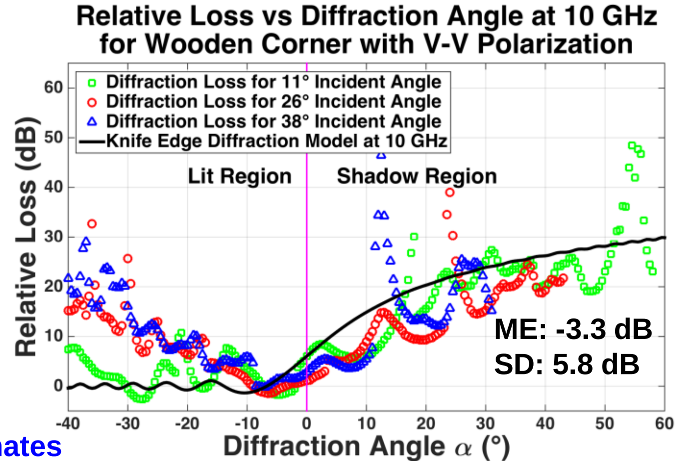

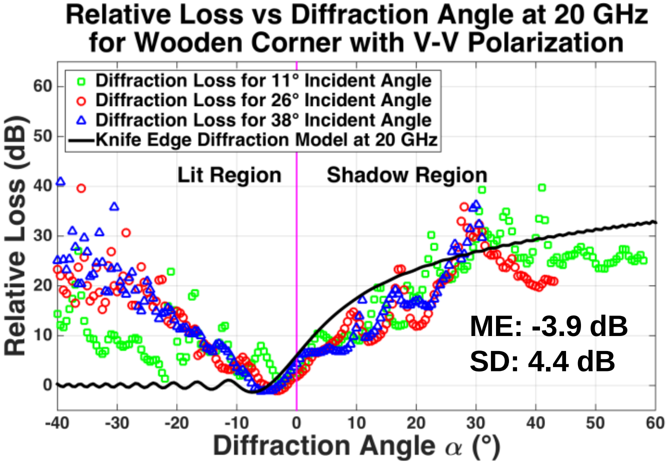

S. Deng, G. R. MacCartney, Jr., and T. S. Rappaport, "Millimeter Wave Diffraction Measurements and Models at 10, 20, and 30 GHz," *2016 IEEE Global Communications Conference (GLOBECOM)*, Dec. 2016.

KED overestimates by 2 – 4 dB

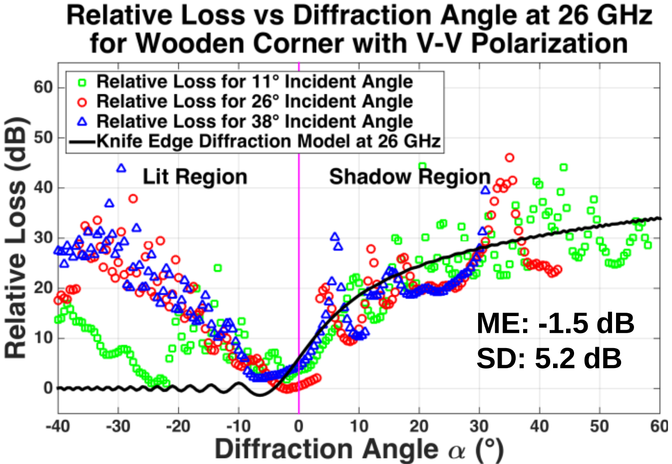

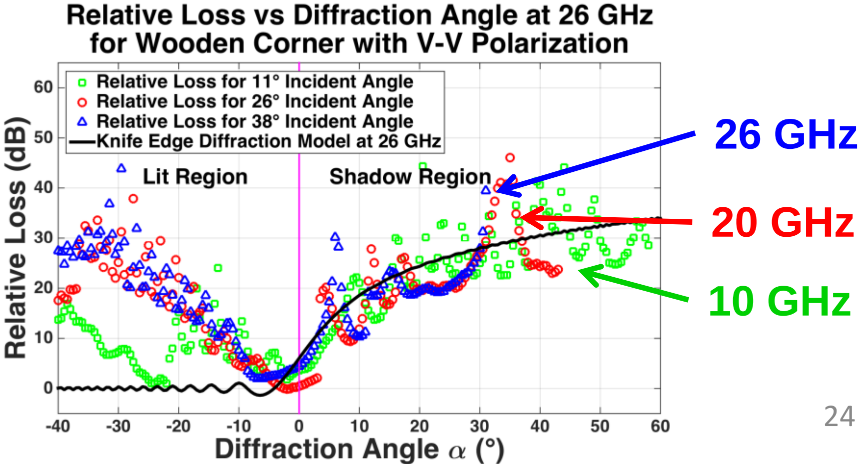

Plastic Board KED Measurements Results

Penetration through the semi-transparent board

KED overestimates by 2 – 4 dB

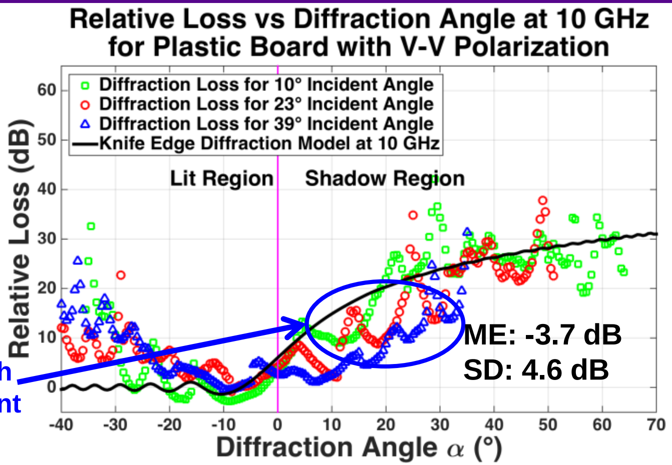

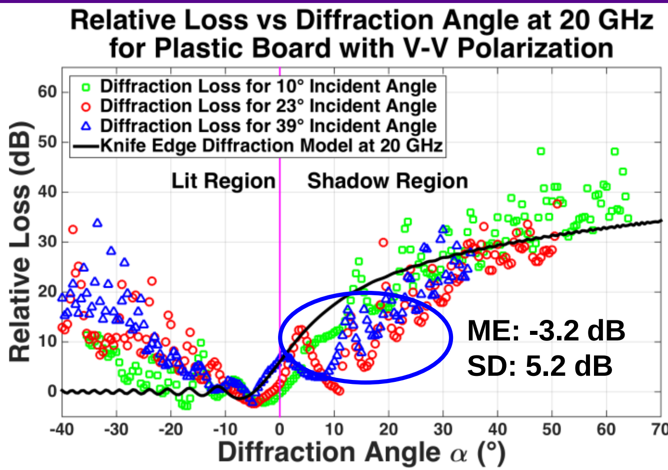

S. Deng, G. R. MacCartney, Jr., and T. S. Rappaport, "Millimeter Wave Diffraction Measurements and Models at 10, 20, and 30 GHz," *2016 IEEE Global Communications Conference (GLOBECOM)*, Dec. 2016.

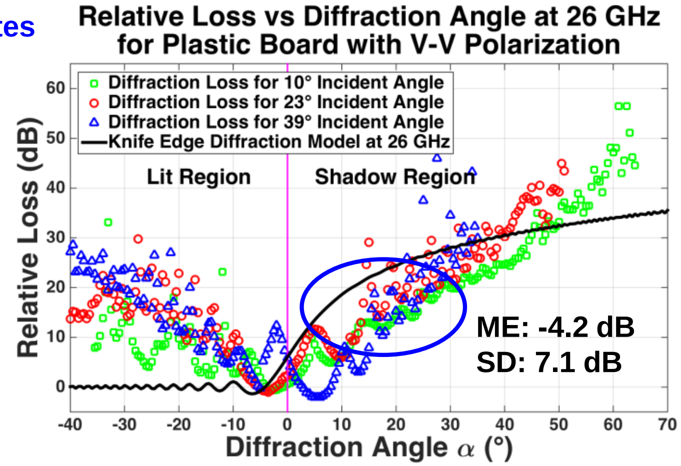

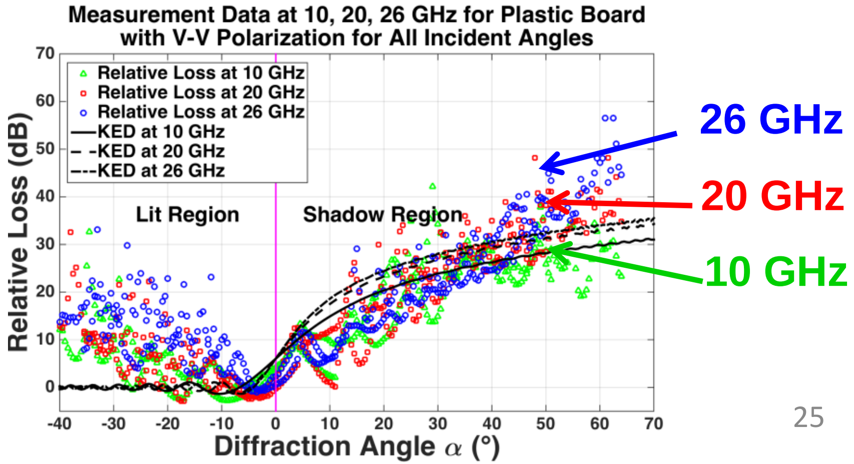

Stone Pillar Creeping Ray Measurements Results

Linear Model
ME: 0.03 dB
SD: 2.8 dB

KED Model
ME: 6.8 dB
SD: 7.5 dB

Anchor point from KED model

n=0.75

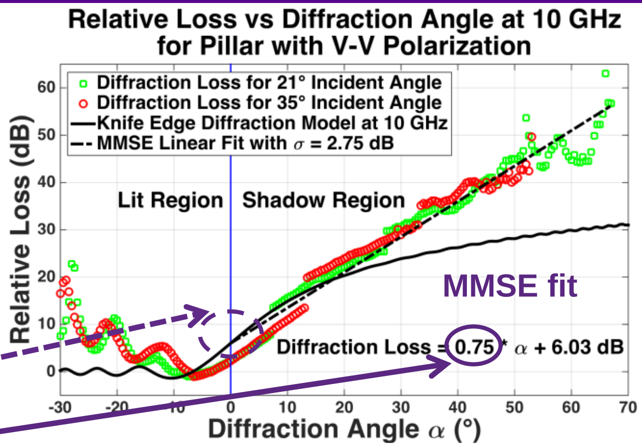

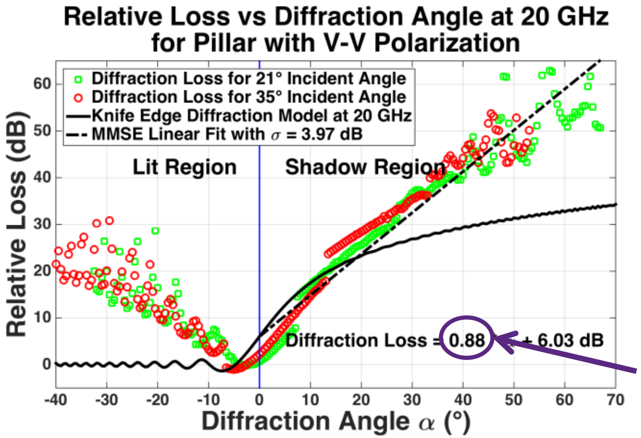

Linear Model
ME: 0.45 dB
SD: 4.3 dB

KED Model
ME: 8.5 dB
SD: 9.2 dB

n=0.88

Linear Model
ME: 0.48 dB
SD: 4.0 dB

KED Model
ME: 9.9 dB
SD: 10.3 dB

n=0.96

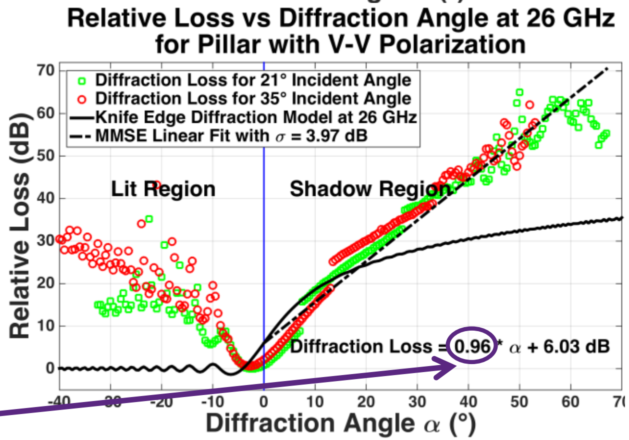

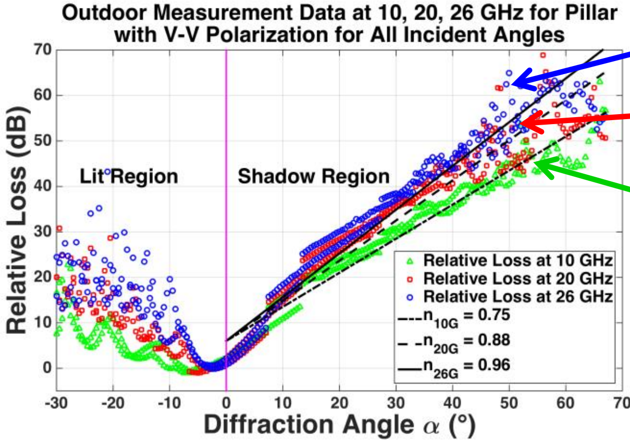

26 GHz

20 GHz

10 GHz

P. A. Tenerelli and C. W. Bostian, "Measurements of 28 GHz diffraction loss by building corners," *IEEE International Symposium on Personal, Indoor and Mobile Radio Communication*, vol.3, pp. 1166-1169, Sept. 1998

Marble Corner Creeping Ray Measurements Results

Linear Model
ME: -0.34 dB
SD: 3.3 dB

KED Model
ME: 1.3 dB
SD: 5.5 dB

n=0.62

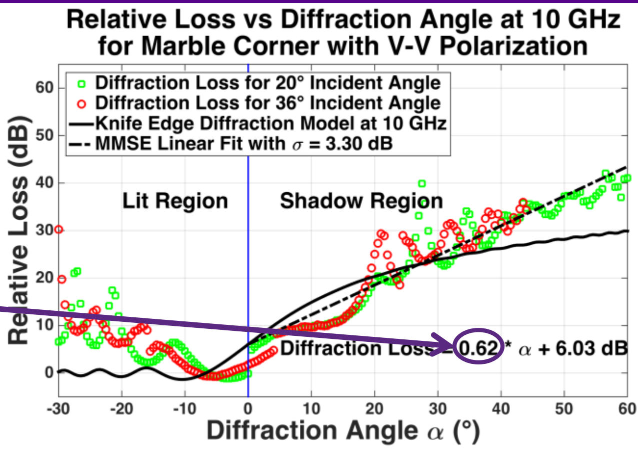

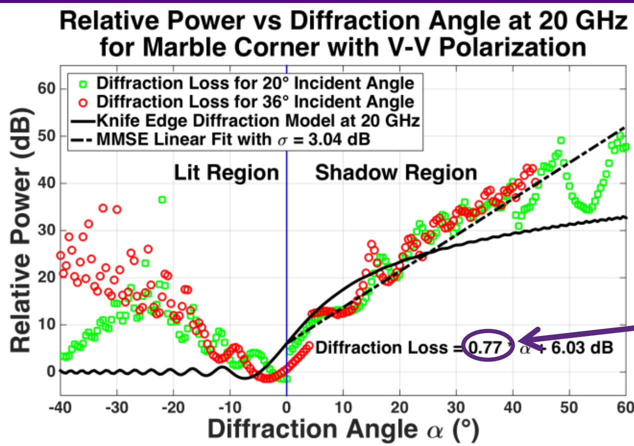

Linear Model
ME: 0.45 dB
SD: 4.3 dB

KED Model
ME: 3.3 dB
SD: 5.8 dB

n=0.77

Linear Model
ME: 4.8 dB
SD: 5.0 dB

KED Model
ME: 7.8 dB
SD: 8.6 dB

n=0.96

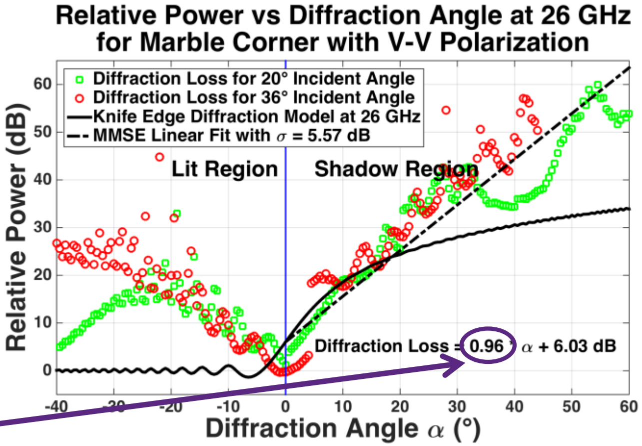

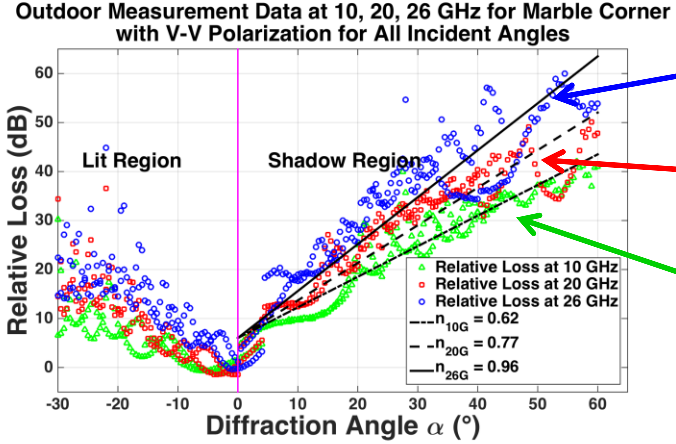

26 GHz

20 GHz

10 GHz

Conclusion

- The KED model can be used in ray tracing tools to calculate diffraction loss in the indoor environment, considering approximately 5-6 dB standard deviations (due to the reflective indoor environment and penetration through the corner).
- The KED model underestimates diffraction loss of outdoor measurements for V-V antenna polarizations, especially in the deep shadow region. The diffraction loss for an outdoor building corner with a rounded edge can be better predicted by a simple linear model.
- The diffraction loss as a function of diffraction angle clearly increased with frequency for identical outdoor measurement locations.
- Typical slope values found in the measurements increased from 0.62 to 0.96.

Spatial Correlation Measurements at 73 GHz

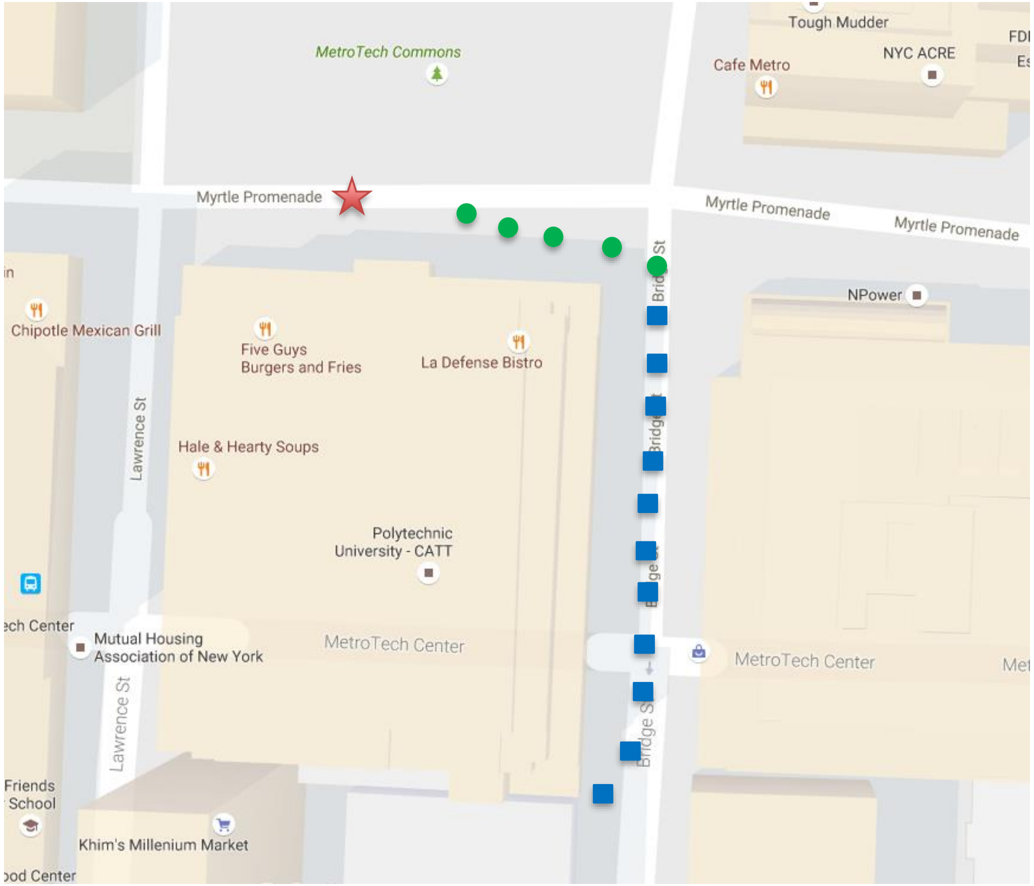

TX: Fixed pointing angle

RX: 5 LOS locations, 11 NLOS locations
5 azimuth sweeps at each RX location

T-R Separation Distance: 30 – 70 m

TX: ★

LOS RX: ●

NLOS RX: ■

Acknowledgment

Acknowledgement to our NYU WIRELESS Industrial Affiliates and NSF

Grants: 1320472, 1302336, and 1555332

NYU TANDON SCHOOL OF ENGINEERING

References

NYU WIRELESS

1. G. R. MacCartney, Jr., S. Deng, S. Sun, and T. S. Rappaport, “Millimeter-Wave Human Blockage at 73 GHz with a Simple Double Knife-Edge Diffraction Model and Extension for Directional Antennas,” *2016 IEEE 84th Vehicular Technology Conference (VTC2016-Fall)*, Sept. 2016.
2. S. Sun, G. R. MacCartney, Jr., M. K. Samimi, and T. S. Rappaport, “Synthesizing omnidirectional antenna patterns, received power and path loss from directional antennas for 5g millimeter-wave communications,” in 2015 IEEE Global Communications Conference (GLOBECOM), Dec. 2015, pp. 1–7.
3. T. S. Rappaport, G. R. MacCartney, Jr., M. K. Samimi, and S. Sun, “Wideband millimeter-wave propagation measurements and channel models for future wireless communication system design (Invited Paper),” IEEE Transactions on Communications, vol. 63, no. 9, pp. 3029–3056, Sept. 2015.
4. T. S. Rappaport, S. Sun, R. Mayzus, H. Zhao, Y. Azar, K. Wang, G. N. Wong, J. K. Schulz, M. K. Samimi, and F. Gutierrez, Jr., “Millimeter Wave Mobile Communications for 5G Cellular: It Will Work!” IEEE Access, vol. 1, pp. 335–349, May 2013.
5. S. Sun, T. S. Rappaport, R. W. Heath, A. Nix, and S. Rangan, “MIMO for millimeter-wave wireless communications: beamforming, spatial multiplexing, or both?” IEEE Communications Magazine, vol. 52, no. 12, pp. 110–121, Dec. 2014.
6. H. Wang and T. S. Rappaport, “A parametric formulation of the UTD diffraction coefficient for real-time propagation prediction modeling,” IEEE Antennas and Wireless Propagation Letters, vol. 4, pp. 253–257, Aug. 2005.
7. R. R. Skidmore, T. S. Rappaport, and A. L. Abbott, “Interactive coverage region and system design simulation for wireless communication systems in multifloored indoor environments: SMT PLUS,” in Proceedings of the 5th IEEE International Conference on Universal Personal Communications, vol. 2, Sept. 1996, pp. 646–650.
8. METIS2020, “METIS Channel Model,” Tech. Rep. METIS2020, Deliverable D1.4 v3, July 2015. [Online]. Available: https://www.metis2020.com/wp-content/uploads/deliverables/METIS_D1.4_v1.0.pdf
9. J. Medbo, J. E. Berg, and F. Harrysson, “Temporal radio channel variations with stationary terminal,” in 2004 IEEE 60th Vehicular Technology Conference (VTC2004-Fall), vol. 1, Sept. 2004, pp. 91–95.
10. J. Medbo and F. Harrysson, “Channel modeling for the stationary ue scenario,” in 2013 7th European Conference on Antennas and Propagation (EuCAP), Apr. 2013, pp. 2811–2815.
11. M. Jacob et al., "A ray tracing based stochastic human blockage model for the IEEE 802.11ad 60 GHz channel model," Proceedings of the 5th European Conference on Antennas and Propagation (EUCAP), Rome, 2011, pp. 3084-3088.

Thank You!

Questions